Two-Phase Downflow Through Catalyst Beds:

E. TALMOR

Chevron Research Company
Richmond, California 94802

Part I. Flow Maps

Flow regimes for nonfoaming and foaming two-phase downflow through catalyst beds are correlated in terms of the superficial volumetric gas-to-liquid ratio and a force ratio relating inertia plus gravity forces to viscous plus interphase forces. In the pulsing flow regime, the frequency of pulses leaving large (29.2 cm) and small (6.58 cm) diameter beds is correlated with the flow map coordinates.

SCOPE

Pulsing has long been recognized as a major flow regime in two-phase downflow through packed beds (Larkins et al., 1961; Weekman and Myers, 1964; Turpin and Huntington, 1967; Charpentier et al., 1969; Beimesch and Kessler, 1971; Sato et al., 1973*a*; Satterfield, 1975). In this flow regime, liquid rich pulses (slugs, waves) traverse the lower portion or the entire length of the bed (within 15 cm from the top), depending on liquid and gas flow rates, physical properties, and packing characteristics. As observed in bed diameters up to 15.2 cm (Turpin and Huntington, 1967), the pulses do not necessarily bridge the entire bed diameter and may have the shape of a wavelike torus (Weekman and Myers, 1964).

As pulsing represents a phase redistribution of a two-phase mixture or a mechanism by which the gas tends to reduce liquid holdup within the bed, related investigations of radial fluid distribution (Weekman and Myers, 1964; Beimesch and Kessler, 1971; Sylvester and Pitayagulsarn, 1975*a*), liquid holdup (Charpentier and Favier, 1975), and mass transfer (Hirose et al., 1974; Sylvester and Pitayagulsarn, 1975*b*) have been conducted. However, before any pulsing related phenomenon or property can be investigated, the boundaries of pulsing in relation to other flow regimes have to be determined.

Until early 1975, published diagrams of flow regime boundaries for two-phase downflow through packed beds have been in terms of superficial mass flow rates of air and water, either G vs. L (Weekman and Myers, 1964; Beimesch and Kessler, 1971; Sato et al., 1973*a*; Satterfield, 1975), L vs. G (Charpentier et al., 1969), or L/G vs. G (Turpin and Huntington, 1967). As such, these diagrams cannot be applied, for example, to petroleum processing units.

A step toward a generalized flow map was published by Charpentier and Favier in late 1975. For the first time, the concept of separate flow maps for nonfoaming and foaming systems was introduced. For nonfoaming systems (water, cyclohexane, gasoline, and petroleum ether with air, nitrogen, helium, and carbon dioxide), the flow map shows three flow regimes: trickling flow (two continuous phases), pulsing, and spray flow (gas continuous). For foaming systems (kerosene, desulfurized and nondesulfurized gas oils with air, nitrogen, helium, and carbon dioxide), the flow map of Charpentier and Favier (1975) identifies four flow regimes: trickling flow, foaming, foaming pulsing flow, and pulsing. Both flow maps show that at constant liquid and gas flow rates, a higher liquid viscosity or a lower liquid surface tension promotes pulsing. However, both flow maps are corrected versions of L/G vs. G plots, where the correction factors for L/G and G are ratios of liquid properties (density, viscosity, and surface tension) to those of water and ratio of gas density to that of air, each property ratio raised to a different power between 0.33 and 1.0. With these empirical corrections, the coordinates of their flow maps have no physical meaning. Furthermore, the range of particle size covered is relatively narrow (0.184 to 0.300 cm), and the prediction of flow regime in hydrogen/hydrocarbon systems relative to water as the liquid phase and air as the gas phase appears questionable.

Therefore, the objective of Part I of this study was to develop a generalized flow map in terms of meaningful coordinates which allow scaling over a wide range of variables. As the need for additional experimental data appeared certain, and because all available data were obtained in small diameter beds (<15.2 cm), a larger diameter bed (29.2 cm) was chosen for acquisition of extra data for mapping and for determination whether increased bed diameter affects pulsing behavior.

CONCLUSIONS AND SIGNIFICANCE

The flow regimes encountered in two-phase downflow through packed beds depend on the superficial volumetric gas-to-liquid ratio and the ratio of inertia plus gravity forces to viscous plus interphase forces. The variables affecting this force ratio are packing size and bed voidage, liquid and gas superficial mass flow rates, densities and viscosities, and liquid surface tension. Bed diameter or height per se do not affect the correlation of flow regimes (Figures 2 and 3).

For nonfoaming systems (Figure 2), the flow map shows five flow regimes: two continuous phases (trickling flow), gas continuous (spray or blurring flow), liquid continuous (dispersed bubble), pulsing, and bubbling/pulsing. For foaming systems (Figure 3), the flow map identifies two continuous phases, gas continuous, foaming, and pulsing with and without foaming; that is, foaming appears in regions where liquid continuous and pulsing are encountered with nonfoaming liquids. In both cases, the correlation is in the form of $(G/L)(\rho_l/\rho_g)_{avg}$ vs. $[1 + (1/Fr)]/[We + (1/Re)]$. Several orders of magnitude variations in the Froude, Weber, and Reynolds numbers are covered using data obtained in this study in a 29.2 cm diameter

bed and data from the literature obtained in smaller diameter beds. Upper and lower boundaries for pulsing show the pulsing flow regime semienclosed by the other flow regimes (Figure 2). Additional significant boundaries are a lower boundary for two continuous phases and a lower boundary for no foaming or bubbling (Figure 3).

Pulse frequency in nonfoaming systems is not affected by bed diameter (Figure 4), and there is a good correspondence between local pulse frequency and local pressure drop oscillation frequency.

The flow regime and pulse frequency correlations (Figures 2 to 4) are useful for analyzing performance of existing or new pilot and commercial reactors.

EXPERIMENTAL

A schematic illustration of the experimental system used in this study is given in Figure 1. The system consisted of a 30.5 cm OD, 0.635 cm wall Plexiglas column packed with 1.22 m of 0.350 cm cylindrical particles, a 0.208 m^3 drum, a circulation pump, and high/low range flowrators for liquid and air flow measurements. The column was provided with a spider type of liquid injector, a chimney distributor right above the packing, and 0.635 cm pressure taps spaced 15.2 cm apart along the packed section. A pressure gauge at the top of the column provided overall pressure drop data, and a 5.08 cm bursting disk in the air line assured that the maximum allowable pressure of 103 421 N/m^2 was not exceeded in the Plexiglas column. Local pressure drops were measured by pneumatic d/p cells mounted above the bed and recorded on a pneumatic consotrol receiver. On those occasions when overall bed pressure drop was measured with a d/p cell, the recorded value was in good agreement with the reading of the pressure gauge.

Water/glycerine solutions of various concentrations (0 to 46%) were prepared in the 0.208 m^3 drum and thoroughly mixed by running the pump on total bypass. As soon as the desired viscosity was reached (by monitoring temperature and specific gravity or by direct measurement of viscosity), the flowrators were calibrated in situ and a liquid flow established through the system by throttling the bypass valve with the block valves of the desired flowrator fully open. In some high flow runs, both high/low flowrators were used in parallel.

Once a desired liquid flow rate was established, air flow was introduced in small increments, and the flow pattern was observed at each air flow while keeping a constant or near constant liquid flow. A series of such runs at constant liquid rate was terminated as soon as the maximum allowable pressure was reached at the top of the column. A new liquid rate would then be established and the flow pattern observed at various increasing air flow rates. All combined, 336 runs were conducted covering a liquid flow range of 2.3 to 34 kg/m^2s, a liquid viscosity range of 0.001 to 0.005 $N \cdot s/m^2$, and an air flow range of 0.033 to 0.68 kg/m^2s.

In some of the runs, pulse frequency was measured at the bottom of the bed. This was done with the help of a stopwatch by visual counting of pulses or waves traversing the bottom 30.5 cm section of the bed or by counting sloshes in the bottom reservoir of the column caused by the pulses. The pulse and slosh counts were in good agreement whenever both were taken for the same run.

FLOW OBSERVATIONS

Depending on liquid flow rate, the starting flow regime at low air rates was either trickling flow (two continuous phases, very little gas-liquid interaction) or dispersed bubble (liquid continuous). In either case, the start of pulsing at some air rate was distinct.

The first pulse always appeared at the bottom of the bed, and the pulse had the appearance of a wave or a wavelike torus rather than a slug. The point of incipient pulsing moved up as the gas rate was increased. However, even when the highest point of incipient pulsing was within 15 cm from the top of the bed, pulses appeared to form at all points below, and a pulse frequency gradient was evident along the bed. With increasing air rate, pulse frequency increased in all bed sections.

Because of the pressure limitation of the Plexiglas column, the air rate could not be increased all the way to the gas continuous flow regime. However, the maximum possible air rate was sufficiently high to increase pulse frequency to a level where it was difficult to distinguish between pulses.

Occasionally, visual observation of low frequency pulses was also difficult. This occurred especially with the richer (33 to 46%) glycerine solutions, where slight foaming (cloudy liquid) obscured the pulses. While not expected with a poorly foaming liquid such as aqueous glycerol, the foaminess of aqueous glycerol, as measured by the time of collapse after shaking (TCS), is reported to be maximum (3 s) at a glycerine concentration of 49% (Bikerman, 1973). The collapse times for the richer (33 to 46%) glycerine solutions used in this study must have, therefore, been below 3 s. This indicates low foaminess, but it was significant enough to obscure pulses and raise overall bed pressure drop.

In the course of flow map development, all aqueous glycerol solutions (0 to 46%) were considered nonfoaming (TCS < 3 s). But, in ascertaining the effect on overall bed pressure drop (Part II), the 33 to 46% glycerine solutions data were separated from the lower concentration (0 to 20%) data.

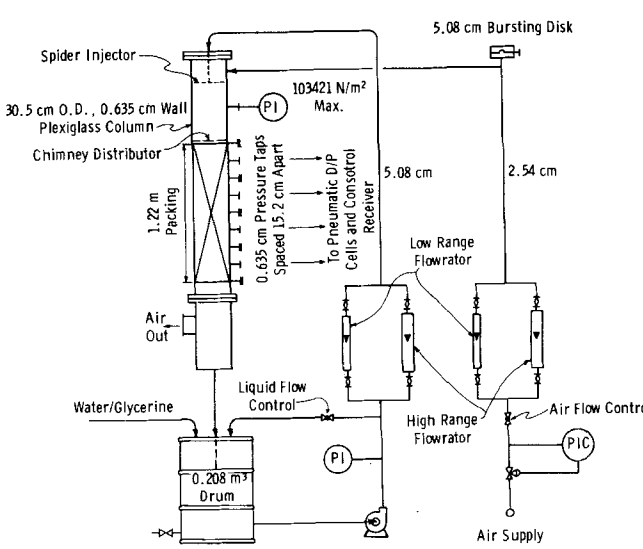

Fig. 1. 30.5 cm OD column flow schematic.

DEVELOPMENT OF FLOW MAP COORDINATES

In the absence of a model for predicting flow regime transitions in two-phase downflow through packed beds, careful consideration should be given to the selection of coordinates for a flow map. The coordinates must have at least some theoretical meaning so as not to be dependent on the particular data used to prepare the map and allow reliable extension to other conditions.

If one seeks guidance from what has been accomplished for two-phase downflow through empty tubes, very little information is available (Oshinowo and Charles, 1974). The bulk of published information is for vertical upflow, and a successful set of coordinates for correlating flow pattern in air/water upflow through empty tubes consists of the superficial volumetric gas-to-liquid ratio and the two-phase superficial Froude number.

Judging by experience in mapping two-phase horizontal and near horizontal flow (Al-Sheikh et al., 1970; Taitel and Dukler, 1976), no two dimensionless groups should be expected to characterize all flow regime transitions and/or correlate all data. Indeed, Oshinowo and Charles (1974) had to modify the superficial two-phase Froude number by empirical property factors to obtain a general representation of flow regimes. As in the case of Charpentier and Favier (1975), the property factors consist of ratios of liquid properties (density, viscosity, and surface tension) to those of water. The factors are raised to different powers between 0.125 and 0.550, and their application as a property modifying group to the two-phase Froude number makes one of the flow map coordinates lose its physical meaning.

However, some guidance for mapping two-phase downflow through packed beds can be derived from the work of Oshinowo and Charles (1974) if one examines the logic or theory underlying a successful correlation of air/water upflow patterns in the form of superficial volumetric gas-to-liquid ratio vs. a superficial two-phase Froude number. The Froude number represents the ratio of inertia-to-gravity forces, and for a two-phase upflow in empty tubes, it also represents a ratio of a main driving force to a main resistance force for the delivery of a given superficial volumetric gas-to-liquid ratio. With this interpretation, the concept of a driving-to-resistance force ratio may be extended to other two-phase systems, provided that all significant driving and resistance forces are properly identified and accounted for.

For two-phase downflow through packed beds, the driving forces are inertia (I) and gravity (G), and the resistance forces are viscous (V) and surface tension (S). Taking the ratio of driving-to-resistance forces and normalizing by the inertia force, we get

$$\frac{\text{Driving Forces}}{\text{Resistance Forces}} = \frac{I+G}{V+S} = \frac{1+(G/I)}{(V/I)+(S/I)} \qquad (1)$$

where G/I, V/I, and S/I are the reciprocals of two-phase Froude, Reynolds, and Weber numbers; that is

$$\frac{\text{Driving Forces}}{\text{Resistance Forces}} = \frac{1+(1/Fr)}{(1/Re)+(1/We)} \qquad (2)$$

Using some of the data of this and other studies (Larkins et al., 1961; Clements and Schmidt, 1976), a plot of the superficial volumetric gas-to-liquid ratio $(G/L)(\rho_l/\rho_g)_{avg}$ vs. the force ratio given by Equation (2) did not yield well-defined boundaries for the pulsing flow regime. The difficulty was mainly due to an improper relative effect of viscosity and surface tension on the force ratio coordinate. In the form of Equation (2), viscosity and surface tension affect the force ratio in the same manner. It appeared that for successful flow mapping, they should have opposite effects on the force ratio. This was accomplished by inverting the term containing the Weber number in Equation (2), that is, by using $[1+(1/Fr)]/[We+(1/Re)]$.

The inversion of the Weber number term in Equation (2) amounts to considering a dynamic resistance force which is inversely proportional to the static surface tension force. Such force is indicative of interaction between phases and should also depend on interface agitation or inertia force.

Specifically, if we define a dynamic interface force as I^2/S and rewrite the force ratio as (inertia + gravity)/(interface + viscous), we have

$$\frac{\text{Inertia + Gravity}}{\text{Interface + Viscous}} = \frac{I+G}{(I^2/S)+V} = \frac{1+(G/I)}{(I/S)+(V/I)} = \frac{1+(1/Fr)}{We+(1/Re)} \qquad (3)$$

where the two-phase dimensionless groups and properties were taken as

$$Fr = \frac{[(L+G)\,v_{lg}]^2}{gD_h}$$

$$We = \frac{D_h(L+G)^2\,v_{lg}}{g_c\sigma_l}$$

$$Re = \frac{D_h(L+G)}{\mu_{lg}}$$

$$v_{lg} = v_l\frac{(L/G)}{1+(L/G)} + v_g\frac{1}{1+(L/G)}$$

$$\mu_{lg} = \mu_l\frac{(L/G)}{1+(L/G)} + \mu_g\frac{1}{1+(L/G)}$$

and

$$D_h = \frac{2\,\epsilon D}{2+3\,(1-\epsilon)\,(D/D_p)}$$

The force ratio given by Equation (3) and the superficial volumetric gas-to-liquid ratio are the coordinates used in this study to map two-phase downflow through packed beds with nonfoaming and foaming liquids.

FLOW MAP FOR NONFOAMING SYSTEMS

Data points from air/water, air/DEG, air/glycerine solutions, carbon dioxide/hexane, natural gas/lube oil, carbon dioxide/lube oil, and Freon 12/silicon oil flowing downward through beds of spheres, cylinders, and Raschig rings are combined in Figure 2 for correlation of nonfoaming flow regimes. Generally, open points represent pulsing runs, and solid points represent nonpulsing runs. For simplicity, no distinction is made between a partially pulsing bed and a fully pulsing bed; both are plotted as pulsing. Similarly, runs described by Larkins et al. (1961) as transitional or slugging are all plotted as pulsing.

The curve surrounding the pulsing flow regime connects the higher and lower pulsing points so as to form upper and lower boundaries for pulsing. In regions of insufficient data, the curve is shown dotted. Similarly, one could draw lower boundaries for the gas continuous and two continuous phases regimes and an upper boundary for the liquid continuous regime which would overlap into the pulsing area; that is, the fringe of pulsing constitutes an overlap area between pulsing and its surrounding flow regimes. Within the overlap area, one would find mostly partially pulsing or nonpulsing data points.

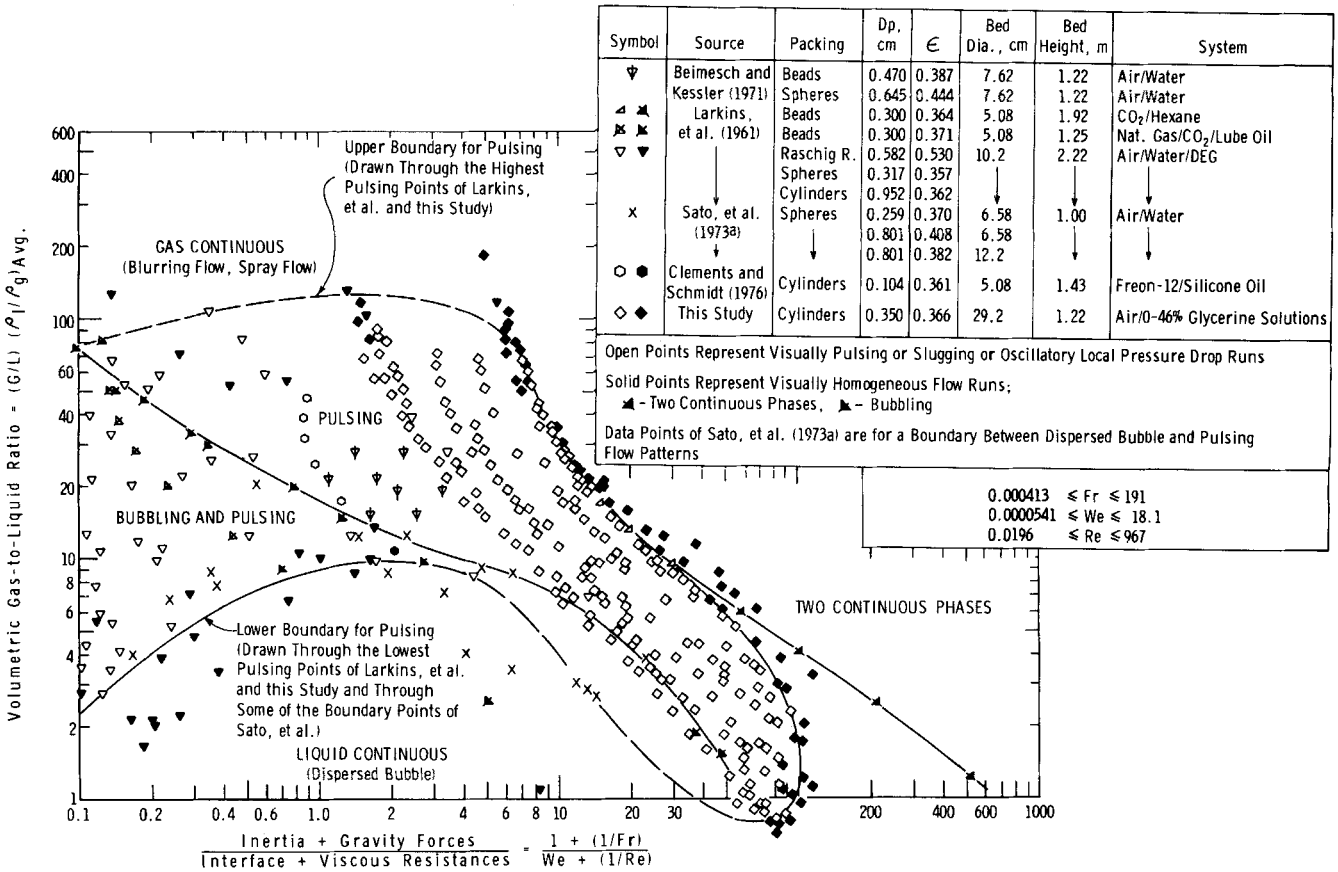

Fig. 2. Flow map for two-phase downflow through packed beds; nonfoaming liquids (TCS <3 s).

As shown (Figure 2), pulsing occurs within a semienclosed area surrounded by a gas continuous regime at high volumetric gas-to-liquid ratios, a two continuous phases regime (trickle flow) at intermediate gas-to-liquid ratios, and a liquid continuous regime at low gas-to-liquid ratios. Within the pulsing area, the map distinguishes between pulsing and bubbling/pulsing. The border between bubbling/pulsing and pulsing is based on natural gas/carbon dioxide/lube oil data (Larkins et al., 1961) and is substantiated by some data of this study obtained with air/33 to 46% glycerine solutions.

The data points of Sato et al. (1973*a*) cannot be characterized as pulsing or not pulsing. They represent borderline points between dispersed bubble and pulsing flow patterns. It is interesting to note that some of these points follow the borderline between bubbling/pulsing and pulsing, and others follow the lower boundary for pulsing. Sato et al. (1973*a*) also reported borderline points between gas continuous and pulsing, but those points could not be used because the operating pressure was not given, and their pressure drop correlation (1973*b*) appears questionable in that region (Part II).

Figure 2 covers several orders-of-magnitude variations of the Froude, Weber, and Reynolds numbers; $0.000413 \leq Fr \leq 191$, $0.0000541 \leq We \leq 18.1$, and $0.0196 \leq Re \leq 967$. The ranges of flow rates and fluid/packing properties covered by Figure 2 are:

L = 0.70 to 200 kg/m^{2}s
ρ_l = 660 to 1 120 kg/m^3
μ_l = 0.33 (10^{-3}) to 41 (10^{-3}) N · s/m^2
σ_l = 0.018 to 0.073 N/m
G = 0.018 to 20 kg/m^{2}s
ρ_g = 0.72 to 6.6 kg/m^3
μ_g = 0.012 (10^{-3}) to 0.018 (10^{-3}) N · s/m^2
D_p = 0.104 to 0.952 cm
ϵ = 0.357 to 0.444
D = 5.08 to 29.2 cm

At a given volumetric gas-to-liquid ratio, the parameters leading to pulsing are increasing liquid rate and viscosity, decreasing surface tension, particle size, and bed voidage. Bed diameter beyond the wall effect range does not affect the flow pattern, and this applies to nonfoaming and foaming systems.

FLOW MAP FOR FOAMING SYSTEMS

Data points for air/silicon oil, air/0.5% methocel solution, and natural gas/kerosene flowing downward through beds of spheres and cylinders are combined in Figure 3 for correlation of flow regimes with foaming liquids. Depending on data source, open points represent visual foaming and pulsing (Clements and Schmidt, 1976) or slugging (Larkins et al., 1961). Solid points represent no foaming (Clements and Schmidt, 1976) or homogeneous flow without pressure surges (Larkins et al., 1961). Foaming appears in regions where liquid continuous and pulsing are encountered with nonfoaming liquids; that is, whereas with a nonfoaming liquid, increasing gas rate at a constant liquid rate leads one from liquid continuous to pulsing and on to gas continuous, with a foaming liquid, the sequence may be foaming, foaming and pulsing, pulsing, and gas continuous.

At some gas-to-liquid ratio, foam may disappear before pulsing. This is shown in Figure 3 by a lower boundary for no foaming or bubbling considerably below the upper

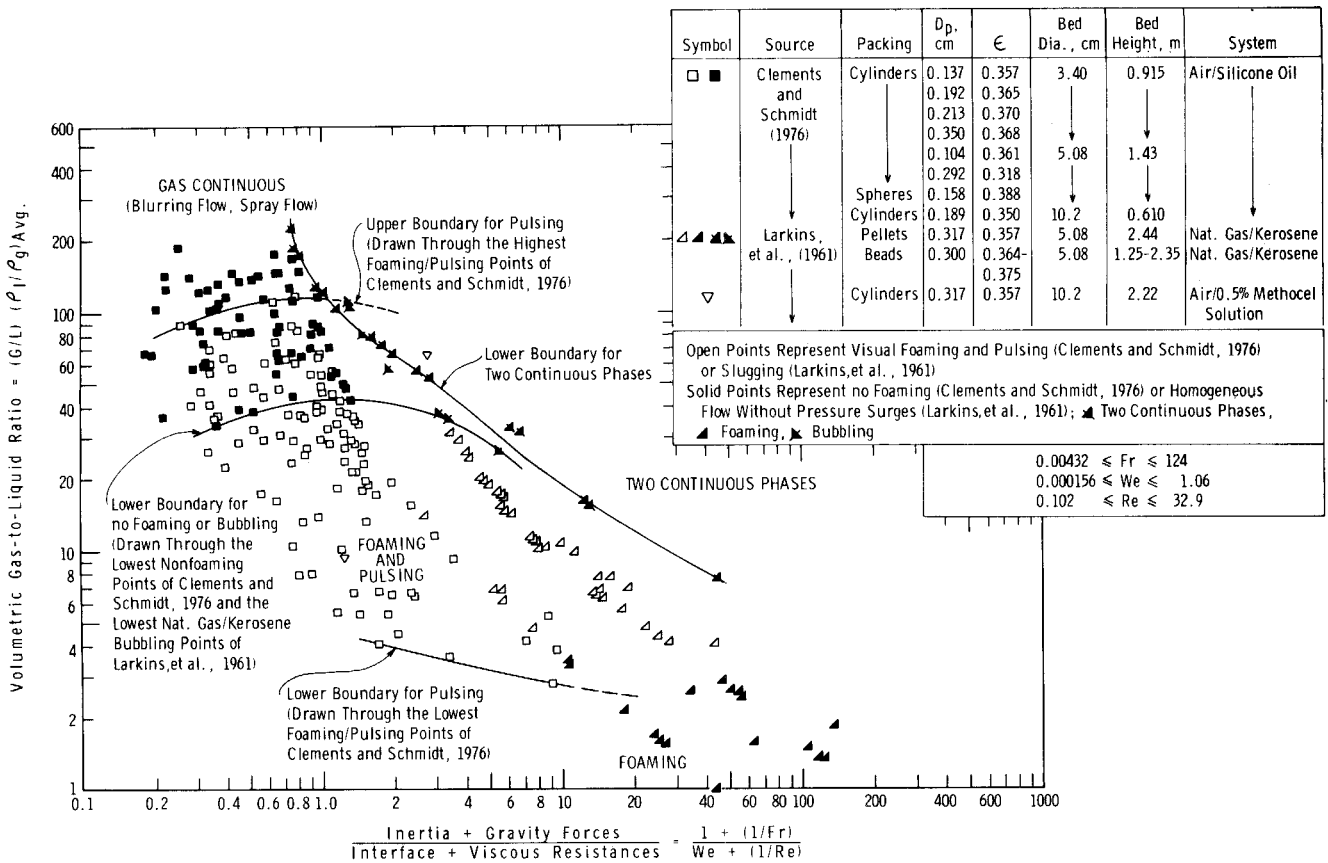

Fig. 3. Flow map for two-phase downflow through packed beds; foaming liquids.

boundary for pulsing. The lower boundary for no foaming is drawn through the lowest nonfoaming points of Clements and Schmidt (1976) and the lowest natural gas/kerosene bubbling points of Larkins et al. (1961). Above the lower boundary for no foaming, no foaming is possible but not certain until above the upper boundary for pulsing. Below the lower boundary for no foaming or bubbling, some unpredictable form of foaming or bubbling should be expected.

Larkins et al. (1961) distinguish between bubbling and foaming. Other investigators do not make such distinction, and indications are that what some call foaming is closer to bubbling. This investigator observed cloudy liquid with air/30 to 46% glycerine solutions. The lack of precision in describing these visual liquid/gas interactions and the lack of a universal measure of foaminess (Bikerman, 1973) make it impossible to predict the type of foam expected at various locations within the foaming and pulsing regions in Figure 3. However, the lower boundary for no foaming appears realistic, particularly in view of the fact that it merges with the lower boundary for two continuous phases. As the latter represents a lower boundary for no interaction between gas and liquid, one should expect it to coincide at least in some range with the lower boundary for no foaming or bubbling; that is, if the two boundaries would not merge, the significance of the lower boundary for no foaming or bubbling would be questionable.

As in the case of Figure 2, Figure 3 covers several orders-of-magnitude variations of the Froude, Weber, and Reynolds numbers: $0.00432 \leq Fr \leq 124$, $0.000156 \leq We \leq 1.06$, and $0.102 \leq Re \leq 32.9$. The ranges of flow rates and fluid/packing properties covered by Figure 3 are:

L = 0.67 to 57 kg/m^{2}s
ρ_l = 800 to 1 000 kg/m^3
μ_l = 1.8 (10^{-3}) to 9.5 (10^{-3}) N · s/m^2
σ_l = 0.018 to 0.053 N/m
G = 0.0013 to 2.7 kg/m^{2}s
ρ_g = 0.53 to 5.0 kg/m^3
μ_g = 0.012 (10^{-3}) to 0.018 (10^{-3}) N · s/m^2
D_p = 0.104 to 0.350 cm
ϵ = 0.318 to 0.388
D = 3.40 to 10.2 cm

Comparison of Figures 2 and 3 suggests that the boundary between two continuous phases and liquid continuous in Figure 2 is an extension of the lower boundary for two continuous phases in Figure 3. It appears that the entire lower boundary for two continuous phases is common to both figures.

PULSE FREQUENCY

Within the pulsing areas, Figures 2 and 3 do not distinguish between various pulse behaviors, for example, various pulse frequencies. To remedy this, the pulse frequency counts taken in this study at the bottom 30 cm section of the 29.2 cm diameter bed were superimposed on the flow map of Figure 2, and curves of constant frequency were drawn through the data (Figure 4).

As shown by the dotted curves in Figure 4, a trough of low frequency (0.3 Hz) is evident within the pulsing area. The frequency increases to at least 1 to 2 Hz by moving away from the trough to either boundary of the pulsing area or by moving along the trough deeper into the pulsing area.

Sato et al. (1973*a*) measured pulse frequency in the bottom 30 cm section of a 6.58 cm diameter bed by counting local pressure drop oscillations from recorded oscillograms. Their results are given in rectangular frames in

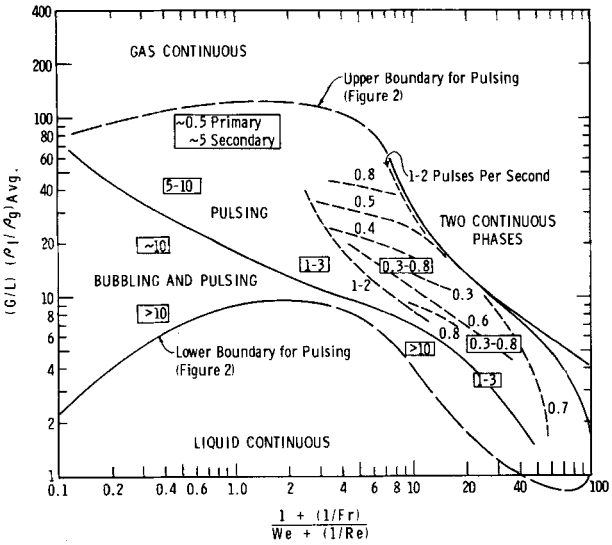

Fig. 4. Pulse frequency contours for two-phase downflow through packed beds; nonfoaming liquids. Contours represent actual counts of pulses per second at bottom 30 cm section of a 29.2 cm diameter, 1.22 m high bed (this study); numbers in frames represent frequency of pressure drop oscillation (s^{-1}) across bottom 30 cm section of a 6.59 cm diameter, 1 m high bed as counted from recorded oscillograms (Sato et al., 1973a).

Figure 4. Note the consistency of pulse frequencies in the small and large diameter beds; that is, increasing bed diameter (at least up to 29.2 cm) does not affect the frequency of pulses leaving the bed. Furthermore, since the consistency is between a large diameter local pulse or wave count and a small diameter local pressure drop oscillation count, the correspondence between local pulse frequency and local pressure drop oscillation frequency reported for small diameter beds (Sato et al., 1973*a*) must also exist in large diameter beds.

Relating the pulse frequency contours of Figure 4 to the various pulsing data sets in Figures 2 and 3, it is evident that all the nonhydrocarbon data of Larkins et al. (1961) and all the air/Freon 12/silicon oil data of Clements and Schmidt (1976) are in the region of extremely high pulse frequency (>5 Hz). This explains the relatively wider scatter of these data and the difficulty in visual observation of pulses, particularly when the high frequency pulsing is combined with foaming or bubbling. In fact, a combination of high frequency pulsing and foaming could lead to the false impression that pulsing and foaming are synonymous.

On the other hand, the data of this study and the hydrocarbon data of Larkins et al. (1961) cover the low pulse frequency region of Figure 4. The lowest measured pulse frequency in that region is 0.3 Hz.

APPLICATION TO COMMERCIAL REACTORS

Figures 2 to 4 have been used to analyze performance of existing reactors and predict flow regime for new units. Use of Figures 2 and 3 for determination of flow regime requires judgment whether the system considered is foaming or nonfoaming. In this regard, the experience of Charpentier and Favier (1975) and Larkins et al. (1961) is worth noting. In presence of gas flow, they found kerosene and desulfurized and nondesulfurized gas oils to be foaming, whereas gasoline, petroleum ether, cyclohexane, hexane, and lube oil did not foam. However, this does not extrapolate to the conditions or actual feedstocks present, for example, in a hydrocracker. If there is any question, both flow maps (Figures 2 and 3) can be consulted.

If a unit falls within the pulsing area, Figure 4 can be used to estimate pulse frequency so as to ensure that proper instrumentation is provided to monitor pulsing if desired. If operation in the pulsing flow regime is not desired, changes to operating or design conditions can be considered which will force the unit out of the pulsing flow regime in accordance with the respective flow map (Figure 2 or 3). Such changes could be a lower superficial liquid flow rate, lower liquid viscosity, larger catalyst particles, or a combination thereof.

A situation which may call for consideration of changes is when the flow map (Figure 2 or 3) shows a new reactor in a different flow regime than the pilot unit which provided the kinetic data for the new reactor design. The fact that the pilot unit and the commercial unit operate in different flow regimes means that catalyst contact efficiency may be different (Satterfield, 1975), and in some cases it may be difficult to predict, even directionally, what the difference may be.

ACKNOWLEDGMENT

Mr. L. D. Clements, presently at Texas Tech University, designed the 30.5 cm OD column system shown in Figure 1 and conducted the first twenty-six runs of this study.

NOTATION

a_p = external surface of a catalyst particle
D = bed diameter
D_h = bed hydraulic diameter, Equation (3)
D_p = effective particle size = $6\ v_p/a_p$
Fr = Froude number, Equation (3)
G = superficial mass velocity of gas
g = acceleration due to gravity
g_c = conversion constant
L = superficial mass velocity of liquid
Re = Reynolds number, Equation (3)
TCS = time of collapse after shaking (Bikerman, 1973)
v = specific volume = $1/\rho$
v_p = volume of catalyst particle
We = Weber number, Equation (3)
ϵ = void fraction of catalyst bed
μ = viscosity
ρ = density
σ_l = liquid surface tension

Subscripts

avg = average for the catalyst bed
l = pertaining to liquid alone
g = pertaining to gas alone
lg = pertaining to two-phase flow

LITERATURE CITED

Al-Sheikh, J. N., D. E. Saunders, and R. S. Brodkey, "Prediction of Flow Patterns in Horizontal Two-Phase Pipe Flow," *Can. J. Chem. Eng.*, 48, 21-29 (1970).

Beimesch, W. E., and D. P. Kessler, "Liquid-Gas Distribution Measurements in the Pulsing Regime of Two-Phase Concurrent Flow in Packed Beds," *AIChE J.*, 17, 1160-1165 (1971).

Bikerman, J. J., *Foams*, p. 104, Springer-Verlag, New York (1973).

Charpentier, J. C., C. Prost, and P. LeGoff, "Chute de pression pour des écoulements á co-courant dans les colonnes á garnissage arrosé: comparaison avec le garnissage noyé," *Chem. Eng. Sci.*, 24, 1777-1794 (1969).

Charpentier, J. C., and M. Favier, "Some Liquid Holdup Experimental Data in Trickle-Bed Reactors for Foaming and Nonfoaming Hydrocarbons," *AIChE J.*, 21, 1213-1218 (1975).

Clements, L. D., and P. C. Schmidt, "Two-Phase Pressure Drop and Dynamic Liquid Holdup in Cocurrent Downflow

in Packed Beds," paper presented at AIChE Annual Meeting, Chicago, Ill. (Nov., 1976).
Hirose, T., M. Toda, and Y. Sato, "Liquid Phase Mass Transfer in Packed Bed Reactor with Cocurrent Gas-Liquid Downflow," *J. Chem. Eng. Japan*, **7**, 187-192 (1974).
Larkins, R. P., R. R. White, and D. W. Jeffrey, "Two-Phase Cocurrent Flow in Packed Beds," *AIChE J.*, **7**, 231-239 (1961).
Oshinowo, T., and M. E. Charles, "Vertical Two-Phase Flow, Part I, Flow Pattern Correlations," *Can. J. Chem. Eng.*, **52**, 25-35 (1974).
Sato, Y., T. Hirose, F. Takahashi, M. Toda, and Y. Hashiguchi, "Flow Pattern and Pulsation Properties of Cocurrent Gas-Liquid Downflow in Packed Beds," *J. Chem. Eng. Japan*, **6**, 315-319 (1973*a*).
Sato, Y., T. Hirose, F. Takahashi, and M. Toda, "Pressure Loss and Liquid Holdup in Packed Bed Reactor with Cocurrent Gas-Liquid Downflow," *ibid.*, 147-152 (1973*b*).
Scatterfield, C. N., "Trickle-Bed Reactors," *AIChE J.*, **21**, 209-228 (1975).
Sylvester, N. D., and P. Pitayagulsarn, "Radial Liquid Distribution in Cocurrent Two-Phase Downflow in Packed Beds," *Can J. Chem. Eng.*, 53, 599-605 (1975*a*).
———, "Mass Transfer for Two-Phase Cocurrent Downflow in a Packed Bed," *Ind. Eng. Chem. Process Design Develop.*, **14**, 421-426 (1975*b*).
Taitel, Y., and A. E. Dukler, "A Model for Predicting Flow Regime Transitions in Horizontal and Near Horizontal Gas-Liquid Flow," *AIChE J.*, **22**, 47-55 (1976).
Turpin, J. L., and R. L. Huntington, "Predictions of Pressure Drop for Two-Phase, Two-Component Concurrent Flow in Packed Beds," *ibid.*, **13**, 1196-1202 (1967).
Weekman, V. W., Jr., and J. E. Myers, "Fluid Flow Characteristics of Concurrent Gas-Liquid Flow in Packed Beds," **10**, 951-957 (1964).

Manuscript received April 25, 1977; revision received July 22, and accepted August 11, 1977.

Part II. Pulsing Regime Pressure Drop

Surveys of local and overall pressure drop in partially pulsing 29.2 cm diameter beds show the overall pressure drop steady but elevated, while local pressure drops across various sections of the bed oscillate in correspondence with the local pulse frequency. The increase in overall pressure drop due to pulsing varies between 0 and 100%, depending on the extent of pulsing and liquid holdup within the bed.

In foaming systems, the overall bed pressure drop can be higher than for pulsing alone, depending on liquid holdup and (apparently) the type of foam and its intensity. In some cases, pulsing appears to be the starting point for low frequency foaming pressure drop surges which are associated with cyclic foam formation and breakup within the bed.

SCOPE

Pressure drop oscillations are often associated with pulsing, and a correspondence between local pulse frequency and local pressure drop oscillation frequency has been observed in beds up to 29.2 cm in diameter and particle sizes in the range of 0.350 to 0.801 cm (Part I of this study; Sato et al., 1973*a*). Yet, the transition into the pulsing flow regime is reported to have no abrupt effect on pressure drop in beds of 5.08, 10.2, and 15.2 cm in diameter packed with 0.762 to 0.823 cm particles (Turpin and Huntington, 1967), whereas manometer fluctuations were greatest at transition into pulsing in 7.62 cm diameter beds packed with 0.378, 0.475, and 0.648 cm beads and spheres (Weekman and Myers, 1964), all operating in the same range of air/water flow rates. Apparently, particle size or some other bed related property controls the extent to which pulsing affects pressure drop. Therefore, the objective of Part II of this study is to determine the extent to which pulsing affects overall bed pressure drop using data from the 30.5 cm OD column system of Part I.

CONCLUSIONS AND SIGNIFICANCE

In the pulsing flow regime, the overall bed pressure drop is not in correspondence with the frequency of pulses leaving the bed. Overall bed pressure drop is relatively steady but elevated, while local pressure drops across various sections of the bed are oscillating in correspondence with local pulse frequency (Figures 1 and 2). The increase in overall pressure drop due to pulsing depends on the extent of pulsing within the bed and the liquid holdup (Figure 3). For fully pulsing beds (Figure 4), the increase in pressure drop goes through a maximum of approximately 100% at liquid holdups [defined by Equation (3)] between 0.5 and 0.6.

When foaming accompanies pulsing, the pressure drop may be higher than for pulsing alone, depending on liquid holdup and (apparently) the type of foam and its intensity (Figure 5).

While foaming may form and exist without pulsing, the latter appears to trigger foaming, which may lead to low frequency foaming pressure drop surges between a pulsing level and a higher pulsing and foaming level. However, the bed pressure drop is not affected by foaming when the liquid holdup [defined by Equation (3)] is below 0.5. In that range, the effect of pulsing per se prevails; that is, pressure drop increases between 0 and 100%, depending on liquid holdup.